Neoplasma 2025; 72(4): 229–241

doi:10.4149/neo_2025_241028N438

Synergistic effects of histone deacetylase inhibitor chidamide and BCL-2 inhibitor venetoclax in activating the p53 pathway in diffuse large B-cell lymphoma

Zhengrong SONG[1], Zhengyan SONG[2], Liyuan REN[3], Xinzhi HAN[1], Xuejun ZHANG[1], Shupeng WEN[1,*]

[1]Department of Hematology, The Second Hospital of Hebei Medical University, Shijiazhuang, Hebei, China; [2]Department of Joint Trauma Surgery, Lincheng County People's Hospital, Xingtai, Hebei, China; [3]Department of Oncology Hematology, Lincheng County People's Hospital, Xingtai, Hebei, China

**Correspondence: Shupengwen0626@163.com*

Received October 28, 2024 / Accepted August 4, 2025

This study aimed to evaluate synergistic effects and molecular mechanisms of the histone deacetylase inhibitor chidamide combined with the BCL-2 inhibitor venetoclax in diffuse large B-cell lymphoma (DLBCL) cell lines. Human DLBCL cell lines (U2932, SUDHL-4) were cultured in vitro and treated with chidamide and venetoclax. Cell proliferation inhibition rates were measured using the CCK-8 assay, and IC50 values were calculated. Cells were also treated with a 5:1 combination of chidamide and venetoclax, along with p53 or p21 siRNA. Cell viability, HDAC activity, apoptosis, cell cycle, the amount of p53 and p21 proteins, and BCL-2-BIM binding were analyzed via CCK-8, enzyme activity assays, the Caspase 3/7 Activity Apoptosis Assay Kit, flow cytometry, RT-qPCR, western blot, and co-IP. The binding of p53 and p21 was verified by dual-luciferase reporter assay and chromatin immunoprecipitation. Chidamide and venetoclax exhibited dose- and time-dependent anti-proliferative effects in U2932 and SUDHL-4 cells, with IC50 values of 3.54 μM (chidamide) and 0.67 μM (venetoclax) in the SUDHL-4 cell line and 5.6 μM (chidamide) and 0.91 μM (venetoclax) in the U2932 cell line. Combination treatment significantly enhanced HDAC inhibition, histone H3/H4 acetylation, and p53 expression, leading to increased cell apoptosis. p53 knockdown partially reversed these effects and increased BCL-2/BIM complex formation. The combination also upregulated p53 expression to increase p21 expression, inducing G1/S phase arrest, which was partially reversed by p21 knockdown. To conclude, the chidamide-venetoclax combination synergistically activates the p53-p21 signaling pathway, leading to cell cycle arrest and apoptosis, representing a potential therapeutic strategy for DLBCL.

Key words: diffuse large B-cell lymphoma; histone deacetylase inhibitor; BCL-2 inhibitor; p53; p21; cell cycle; apoptosis; synergy

Diffuse large B-cell lymphoma (DLBCL) is the most prevalent and aggressive form of non-Hodgkin lymphoma, known for its significant heterogeneity and poor prognosis [1, 2]. Despite advancements in treatment, with rituximab, cyclophosphamide, doxorubicin, vincristine, and prednisone regimen being the standard first-line treatment paradigm, approximately 30–40% of patients with DLBCL still experience relapse or become resistant to treatment [3]. This substantial rate of treatment failure highlights the urgent need for novel therapeutic approaches. In recent years, the role of epigenetic regulation in cancer progression has garnered growing attention, particularly the abnormal activity of histone deacetylases (HDACs), which has been linked to the pathogenesis of several cancers [4–6]. As a result, HDAC inhibitors (HDACis) have emerged as promising agents for the treatment of various hematologic malignancies, including DLBCL [7, 8].

Chidamide, a novel HDACi, exerts its anti-tumor effects by modulating gene expression, inhibiting cell proliferation, and promoting apoptosis in cancer cells [9, 10]. While chidamide has demonstrated therapeutic potential in several malignancies, its precise mechanisms of action in DLBCL remain incompletely understood. In DLBCL, HDACs are highly expressed and frequently mutated, contributing to tumor progression. Chidamide has been found to counteract rituximab-induced downregulation of CD20, restoring

CD20 surface expression and thereby enhancing rituximab-mediated cytotoxicity [11]. Furthermore, chidamide's effects on DLBCL include modulation of key pathways such as PI3K/AKT and mTOR, as well as promoting apoptosis and inhibiting cell proliferation [12]. These findings indicate that chidamide may be a promising adjuvant for relapsed or refractory DLBCL.

Additionally, DLBCL is characterized by the dysregulation of the BCL-2 protein family, which is crucial for promoting cell survival and contributing to resistance to apoptosis [13]. The overexpression of BCL-2 in DLBCL creates an environment where cancer cells are more resistant to apoptosis, making the disease particularly difficult to treat [14]. Venetoclax, a selective BCL-2 inhibitor, has shown promise in targeting this pathway by binding to BCL-2 and triggering apoptosis, leading to clinical efficacy in certain hematologic cancers [15, 16]. However, given the complexity and heterogeneity of DLBCL, single-agent therapies, including venetoclax, often provide limited results, especially in patients with relapsed or refractory disease [17]. Thus, combination therapies are increasingly being explored as a means to enhance treatment efficacy and overcome resistance [18–20]. Despite these advances, the chidamide-venetoclax combination in DLBCL remains largely unexplored.

Based on these challenges, the central scientific question of this study is whether the combination of chidamide and venetoclax can synergistically inhibit DLBCL cell proliferation and enhance the sensitivity of these cells to therapy. Furthermore, we aim to uncover the molecular mechanisms underlying this potential synergy and propose a new strategy for the treatment of DLBCL.

Materials and methods

***In vitro* culture of DLBCL cell lines.** Human DLBCL cell lines U2932 (ABC subtype) (Procell, #CM-0838), SUDHL-4 (GCB subtype, $MYC^+/BCL\text{-}2^+$) (Procell, #CL-0692), and human HEK293T cells (Procell, #CL-0001) were obtained from Procell (Wuhan, China). U2932 and SUDHL-4 cells were cultured in RPMI-1640 medium (Gibco, #11875093), while HEK293T cells were cultured in Dulbecco's Modified Eagle Medium (DMEM) (Gibco, #10564011). Both RPMI-1640 and DMEM media were supplemented with 10% fetal bovine serum (Ausgenex, C0227), 100 U/ml penicillin, and 100 mg/l streptomycin (Gibco, #15140122). Cells were maintained in a humidified incubator at 37 °C with 5% CO_2 and were passaged every 48-72 h.

Cell treatment and grouping. DLBCL cells were exposed to varying concentrations of chidamide (2.5, 5.0, 7.5, 10, or 12.5 μmol/l) and/or venetoclax (0.05, 0.1, 0.5, 1, or 2.5 μmol/l). Subsequently, a CCK-8 assay was performed to assess the inhibition rate of cell proliferation. Drug sensitivity curves were plotted using GraphPad 9.5 software to calculate the half maximal inhibitory concentration (IC_{50}) values. Using the lower IC_{50} concentration for each drug, chidamide and venetoclax were combined in a fixed ratio of 5:1 for subsequent combination treatments [21].

Small interfering RNAs (siRNAs) used in this study were obtained from Cell Signaling Technology (p53, #6231; p21, #6456; Control siRNA, #6568). Following the manufacturer's protocol, cells were transfected with p53 siRNA, p21 siRNA, or negative control siRNA (NC) using Lipofectamine 2000 (Thermo Fisher, #11668030). After 24 h, cells were treated with the chidamide and venetoclax combination.

Cell groups: Blank, Chidamide, Venetoclax, Chidamide + Venetoclax, si-NC+Chidamide + Venetoclax, si-p53 + Chidamide + Venetoclax, si-p21 + Chidamide + Venetoclax.

CCK-8 cell viability assay. Logarithmically growing U2932 and SUDHL-4 cell lines were seeded into 96-well plates at 100 μl of medium per well, in triplicate for each group. Cells were seeded into 96-well plates at various cell densities (10,000; 8,000; and 5,000 cells/well) according to different time points (24, 48, and 72 h). On the following day, cells were treated with the drugs, and at 24 h, 48 h, and 72 h post-treatment, 10 μl of CCK-8 reagent (Beyotime, #C0038) was added to each well to assess the cell proliferation inhibition rate. After incubation in the dark for 2–3 h, the optical density (OD) was measured at 450 nm using a microplate reader (Biotek, Synergy HTX, Winooski, VT, USA). The cell proliferation inhibition rate was calculated using the formula: Cell proliferation inhibition rate (%) = (OD value of control group – OD value of experimental group) / (OD value of control group – OD value of blank group) × 100%.

CompuSyn 1.0 software [22] was used to perform combination analysis of chidamide and venetoclax at various doses, quantifying the combination index (CI) to evaluate drug synergism.

Caspase 3/7 activity apoptosis assay. U2932 and SUDHL-4 cells were treated in the same cell number and drug administration as the CCK-8 cell viability assay. Cell apoptosis was assessed using the Caspase 3/7 Activity Apoptosis Assay Kit (Solarbio, Beijing, China; #CA1060). Absorbance values at an excitation wavelength of 485 nm and an emission wavelength of 515 nm were measured using a microplate reader (Biotek).

HDAC fluorescence activity assay. Cells were treated with chidamide and venetoclax for 24 h, after which HDAC activity in the cell lysates was assessed using an HDAC fluorescence activity assay kit (Abcam, #ab1432). A total of 50 μg of cell lysate was incubated with the fluorescent substrate at 37 °C for 30 min. After incubation, the lysine developer provided in the kit was added to terminate the reaction, followed by 30 min incubation at 37 °C. Fluorescence was then measured at 405 nm using a microplate reader (Biotek).

Flow cytometric analysis of apoptosis and cell cycle. Cell apoptosis following 24 h treatment with chidamide and/or venetoclax was analyzed using an Annexin V-FITC/PI apoptosis detection kit (KeyGen, China). Following the manufacturer's instructions, cells were washed with PBS, digested with trypsin without EDTA, and resuspended in

100 µl of 1× Binding Buffer. The cells were then incubated in the dark for 15 min with 5 µl of Annexin V-FITC and 5 µl of PI.

For cell cycle analysis, following 24 h treatment with chidamide and/or venetoclax, cells were fixed overnight in 70% ethanol at 4 °C. The next day, cells were washed twice with PBS, treated with RNaseA for 30 min at 4 °C, and stained with PI (KeyGen, China) for 30 min at 4 °C.

Samples were analyzed using a BD FACSCanto II flow cytometer (Becton Dickinson, USA), and data on apoptosis and cell cycle phases were processed using FlowJo software (FlowJo, USA).

Quantitative real-time reverse transcription polymerase chain reaction (qRT-PCR). Total RNA was isolated from cells using a Total RNA Isolation kit (Axygen, NY, USA, #AP-MN-MS-RNA-250) and reverse-transcribed into complementary DNA (cDNA) using the Primescript RT reagent kit (Takara, Dalian, China, #RR037Q). cDNA was quantified by qRT-PCR, and the data were acquired with SYBR Premix Ex TaqTM II (Takara, #RR390Q) using ABI7900HT Fast Real-Time PCR system (Applied Biosystems, Foster City, CA). The PCR reaction conditions consisted of 10 min pre-denaturation at 95 °C; 40 cycles of 10 s denaturation at 95 °C, 20 s annealing at 60 °C, and 34 s extension at 72 °C. β-actin was used as an internal control, and the fold changes were calculated by the $2^{-\Delta\Delta Ct}$ method. The primers are listed in Table 1.

Western blot analysis. Cells were lysed with radioimmunoprecipitation assay (RIPA) lysis buffer (#P0039, Beyotime) containing a protease inhibitor cocktail (#P1006, Beyotime), mixed thoroughly, and incubated on ice for 30 min. The lysate was then centrifuged at 13,000 × g for 10 min, and the supernatant was collected. The protein concentration was subsequently measured using a BCA protein assay kit (Beyotime, #P0010). Samples of the cell protein were loaded and separated via sodium dodecyl sulfate-polyacrylamide gel electrophoresis (SDS-PAGE). Following electrophoresis, the proteins were transferred to a PVDF membrane (Millipore, #IPVH 20200). The membrane was blocked with 5% non-fat milk at room temperature for 2 h. Diluted primary antibodies were then added, including rabbit anti-β-actin (CST, #4970), rabbit anti-Ac-H3 (AC-K9, CST, #9649), rabbit anti-Ac-H4 (AC-K8, CST, #2594), mouse anti-p53 (Abcam, #ab26), rabbit anti-BCL-2 (CST, #3498), rabbit anti-BAX (CST, #5023), rabbit anti-cleaved caspase 3 (Abcam, #ab32042), rabbit anti-BIM (Abcam, #ab32158), rabbit anti-p21 (CST, #2947), rabbit anti-Cyclin E (CST, #20808), and rabbit anti-Cdk2 (Abcam, #ab32147). The membrane was incubated overnight at 4 °C. After washing, HRP-conjugated secondary antibodies, goat anti-rabbit IgG (Servicebio, GB23303) or goat anti-mouse IgG (Abcam, #ab205719), were added and incubated at room temperature for 1 h. Detection was performed using ECL detection reagents (Millipore, #WBKLS0500). Bands in the western blot images were quantified using Image Pro Plus 6.0 (Media Cybernetics, USA), with β-actin as a loading control. Each experiment was conducted in triplicate.

Co-immunoprecipitation (co-IP) assay. Cells were lysed with RIPA lysis buffer (Beyotime, P0039) containing protease inhibitor cocktail (Beyotime, #P1006), thoroughly mixed, and lysed on ice for 30 min. The lysate was centrifuged at 13,000 × g for 10 min, and the supernatant was collected as the cell lysate. Next, 50 µl of the cell lysate was used for the western blot analysis to determine BCL-2 and BIM proteins in the Input sample. The 50 µl cell lysis buffer was incubated with anti-BCL-2 (CST, #3498) or negative control IgG (Abcam, #ab313801) at 4 °C overnight and then with PureProteome™ Protein A/G Mix Magnetic Beads (Merck Millipore, Burlington, MA, USA) for 2 h. Following centrifugation, supernatants and agarose beads were separated and collected. Subsequently, the agarose beads were washed with ice-cold PBS, and the bound proteins were eluted. After centrifugation, precipitated proteins were then subjected to western blot analysis to examine BCL-2 and BIM protein levels.

Dual luciferase reporter assay. Using the Jaspar database (https://jaspar.elixir.no/), we identified a predicted binding site for p53 at the p21 promoter, specifically 5'-AACATGTCCCAACATGTT-3' (NC_000006.12). This sequence was amplified and cloned into the pGL3-Basic vector to generate the promoter-reporter gene plasmid pGL3-p21-WT. Additionally, the sequence was mutated to 5'-AACAAAAAAAAAAATGTT-3' to construct the mutant plasmid pGL3-p21-MUT, and all constructed plasmids were validated by sequencing. HEK293T cells were seeded in 24-well plates. The pGL3-p21-WT/pGL3-p21-MUT, along with the phRL-TK (as a control), were transiently transfected into p53-overexpressing cells using the plasmid pCMV-3X Flag-p53 (Beyotime, #D3031). After 48 h of incubation, luciferase activity was assessed using a dual luciferase reporter assay kit (Promega, #E1910).

Chromatin immunoprecipitation (ChIP) assay. U2932 and SUDHL-4 cells, treated with drugs for 24 h, were cross-linked at room temperature with 1% formaldehyde for 10 min, followed by quenching with glycine to a final concentration of 0.125 M. After two washes with PBS, the cells

Table 1. Primer sequences for qRT-PCR.

Gene	Forward 5'–3'	Reverse 5'–3'
p53	ACCTATGGAAACTACTTCCTGAAA	CTGGCATTCTGGGAGCTTCA
p21	AGGAGACAGACAACTCACTCG	CATGGCGCCTGAACAGAAGA
β-actin	GAGAAAATCTGGCACCACACC	GGATAGCACAGCCTGGATAGCA

were collected and resuspended in ChIP lysis buffer (50 mM HEPES-KOH, pH 7.5; 140 mM NaCl; 1 mM EDTA, pH 8; 1% Triton X-100; 0.1% sodium deoxycholate; 0.1% SDS; and 1% protease inhibitor). Following 10 min incubation on ice, the nuclei were collected, resuspended in ChIP lysis buffer, and sonicated to obtain DNA fragments of 50–200 base pairs. Magnetic beads coated with p53-specific antibody (Abcam, #ab26) or IgG (negative control) were then added to the lysate and incubated overnight. The following day, the beads were washed seven times with washing buffer (50 mM HEPES, pH 7.5; 500 mM LiCl; 1 mM EDTA; 1% NP-40; and 0.7% sodium deoxycholate) and once with TE buffer (10 mM Tris, pH 8.0; 1 mM EDTA). The protein-DNA complexes were then eluted from the beads. Finally, specific primers for p21 were used to perform PCR on the purified DNA, with the following sequences: Forward: 5'-GTGTCTGCTGCAAATCTCA-3', Reverse: 5'-TCTTCCTGTTCCTGGCTC-3'. The amplification conditions were as follows: pre-incubation at 95 °C for 120 s, followed by 40 cycles of 95 °C for 30 s, 60 °C for 30 s, and 72 °C for 30 s, with a final extension at 72 °C for 5 min. The presence of target gene sequences was assessed to determine potential interactions between the target protein and the gene.

Statistical analysis. All data were processed using GraphPad 9.5 software (San Diego, CA, USA). Quantitative data are expressed as mean ± standard deviation. A t-test was employed for comparisons between two groups, whereas one-way ANOVA was applied for comparisons among multiple groups. A p-value of <0.05 was deemed statistically significant, denoted by an asterisk (*).

Results

Synergistic effects of chidamide and venetoclax on DLBCL cells. To determine the sensitivity of U2932 and SUDHL-4 cell lines to chidamide and venetoclax, we treated these cells with various concentrations of chidamide (0, 2.5, 5.0, 7.5, 10, or 12.5 μmol/l) and/or venetoclax (0, 0.25, 0.5, 0.75, 1, or 1.25 μmol/l). Cell viability was measured using the CCK-8 assay at 24, 48, and 72 h, as illustrated in Figure 1A. The single-agent treatment demonstrated a dose- and time-dependent inhibitory effect on both cell lines. Specifically, the IC_{50} values for chidamide and venetoclax after 24 h of treatment in U2932 cells were 5.6 μM and 0.91 μM, respectively, while in SUDHL-4 cells, the IC_{50} values were 3.54 μM and 0.67 μM, respectively, as detailed in Figure 1B.

Next, we evaluated the impact of the combination of both drugs on U2932 and SUDHL-4 cells after 24 h. Using the Chou-Talalay method for drug combination, we established a constant ratio of 5:1 for chidamide and venetoclax using several concentration points above or below the 24 h IC_{50} values in a two-fold dilution series [21]. The results indicated that the combined treatment had a greater inhibitory effect than either single-agent treatment (Figure 1C). Furthermore, we performed graphical analysis of the CI values following the Chou-Talalay method; the drugs' combined effect is synergistic at concentrations that induce no more than a 50% effect on viability; if the fraction affected is >50%, the effect is additive and then inhibitory, as shown in Figure 1D. At 50% cell proliferation [fraction affected (Fa) = 0.5], the CI values for SUDHL-4 and U2932 cell lines were 0.87 and 0.89, respectively, suggesting a synergistic interaction between the two drugs (CI <1). Meanwhile, we also employed the Caspase 3/7 Activity Apoptosis Assay Kit to evaluate cell apoptosis. Consistent with the CCK-8 results, single-agent treatment with chidamide or venetoclax exhibited pro-apoptotic effects on the two cells in a dose- and time-dependent manner (Figure 1E); as expected, the combined treatment with chidamide and venetoclax showed a superior promoting effect to the single-agent treatment (Figure 1F).

Chidamide combined with venetoclax inhibits HDAC activity, enhancing acetylation of histones H3/H4. To elucidate the impact of the chidamide and venetoclax combination on HDAC activity in tumor cell lines, we treated U2932 cells with 5 μmol/l of chidamide and/or 1 μmol/l of venetoclax, while SUDHL-4 cells were treated with 2.5 μmol/l of chidamide and/or 0.5 μmol/l of venetoclax for 24 h. As shown in Figures 2A and 2B, chidamide or venetoclax single treatment reduced DLBCL cell viability and augmented cell apoptosis; however, these alterations were more pronounced following combined treatment with chidamide and venetoclax relative to single treatment (all $p<0.001$). Subsequent assessments of HDAC activity were conducted using an HDAC activity assay kit. As illustrated in Figure 2C, treatment with chidamide resulted in a significant inhibition of HDAC activity compared to treatment with venetoclax, but there was no significant difference. Notably, the combination treatment exhibited a more pronounced inhibitory effect on HDAC activity in tumor cells compared to chidamide or venetoclax administered alone (all $p<0.05$).

Evidence has shown that HDAC enzymes can inhibit the acetylation of histone H3 and histone H4 [23]. Here, the current results of western blot analysis demonstrated that treatment with chidamide significantly increased acetylation of histone H3 at the Lys9 position and histone H4 at the Lys8 position in comparison with treatment with venetoclax. Furthermore, the combination treatment with chidamide or venetoclax resulted in even greater increases in acetylation levels of histone H3 and histone H4 than treatment with either single agent (all $p<0.05$) (Figure 2D). These results indicate that the HDACi chidamide promotes the acetylation of lysine residues on histones H3 and H4. The concomitant use of venetoclax appears to amplify the therapeutic efficacy of chidamide in this context.

Chidamide combined with venetoclax induces apoptosis in DLBCL through upregulation of p53. To clarify the molecular mechanisms that contribute to the synergistic enhancement of drug sensitivity in DLBCL cells by chidamide and venetoclax, we employed flow cytometry to assess apoptosis across the experimental groups.

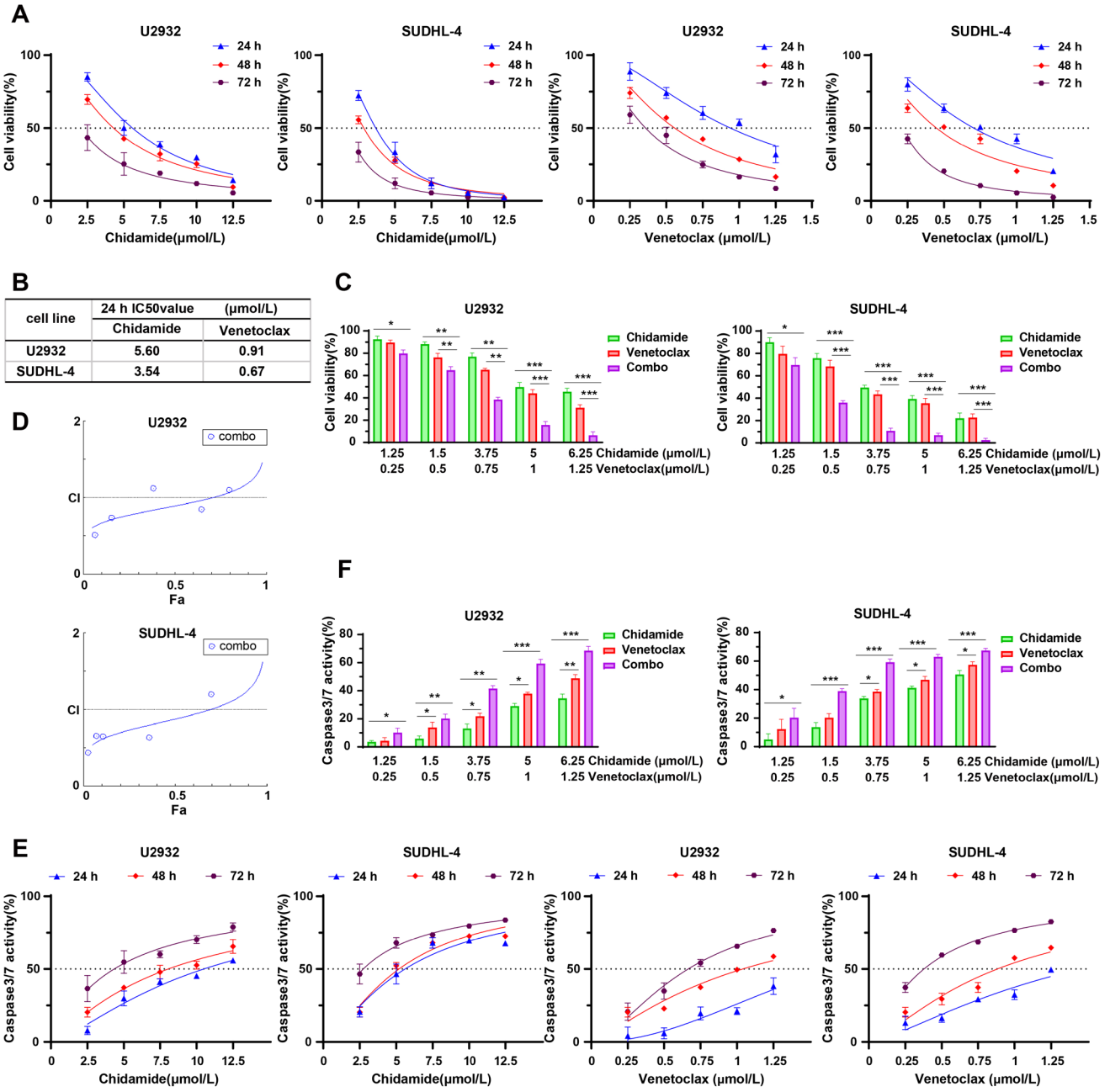

cell line	24 h IC50value	(μmol/L)
	Chidamide	Venetoclax
U2932	5.60	0.91
SUDHL-4	3.54	0.67

Figure 1. Effects of chidamide and venetoclax on DLBCL cells. A, E) U2932 and SUDHL-4 cell lines were exposed to chidamide (2.5, 5.0, 7.5, 10, or 12.5 μmol/l) or venetoclax (0.25, 0.5, 0.75, 1, or 1.25 μmol/l) for 24, 48, or 72 h. Cell viability was assessed using the CCK-8 assay, and cell apoptosis was evaluated by the Caspase 3/7 Activity Apoptosis Assay Kit. B) IC_{50} values at 24 h were calculated based on the cell viability analysis. C, F) U2932 and SUDHL-4 cells were treated for 24 h with a drug combination at a constant ratio of 5:1 (chidamide:venetoclax). Cell viability was measured using the CCK-8 assay, and cell apoptosis was evaluated by the Caspase 3/7 Activity Apoptosis Assay Kit. D) Graphical analysis of CI values was performed according to the Chou-Talalay method. Cell experiments were performed independently in triplicate, and data are expressed as mean ± standard deviation. Abbreviations: DLBCL-Diffuse Large B-Cell Lymphoma; CCK-8-Cell Counting Kit-8; IC_{50}-Half Maximal Inhibitory Concentration; CI-Combination Index; Caspase 3/7-cysteine aspartase 3/7

As illustrated in Figure 3A, treatment with chidamide or venetoclax significantly increased apoptosis in DLBCL cells, and the latter caused more profound effects. Notably, apoptosis levels were markedly increased following the combined treatment compared to single-agent therapy (all $p<0.001$). Western blot analysis revealed that treatment with chidamide and venetoclax led to elevated expression levels of apoptosis-related proteins p53, BAX, and cleaved caspase

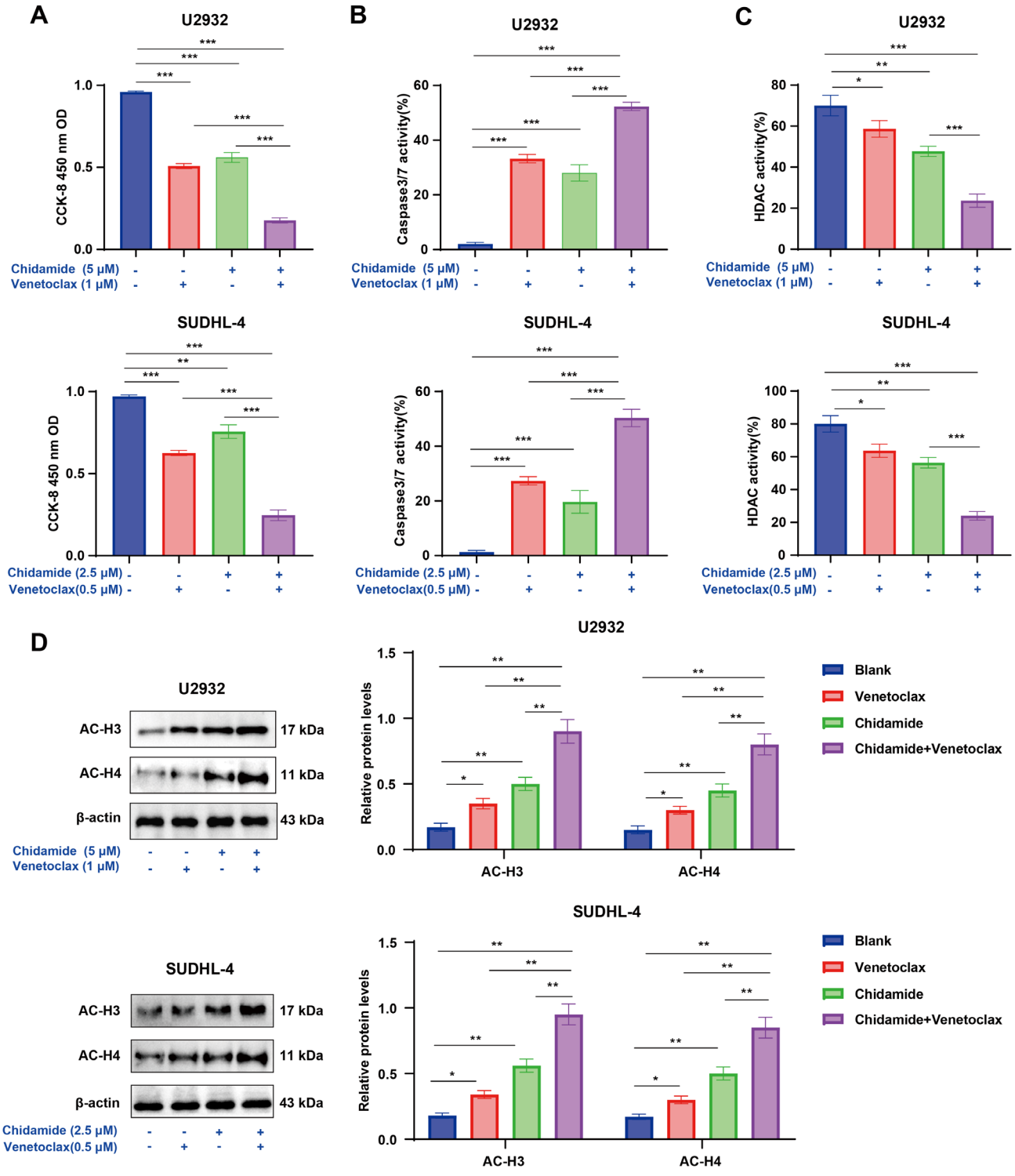

Figure 2. Effects of chidamide combined with venetoclax on HDAC activity and histone H3/H4 acetylation in DLBCL cells. A) Cell viability was assessed using the CCK-8 assay. B) Cell apoptosis was evaluated by the Caspase 3/7 Activity Apoptosis Assay Kit. C) Assessment of HDAC activity was performed using an HDAC activity assay kit. D) Western blot analysis was conducted to evaluate the acetylation of lysine residues in histones H3 and H4. All cellular experiments were conducted in triplicate independently, and the data are presented as mean ± standard deviation. Comparisons among groups were analyzed using one-way ANOVA, followed by Tukey's multiple comparisons test. Statistical significance is indicated as *p<0.05, **p<0.01, and ***p<0.001. Abbreviations: HDAC-Histone deacetylase; AC-H3-Acetylated histone H3; AC-H4-Acetylated histone H4

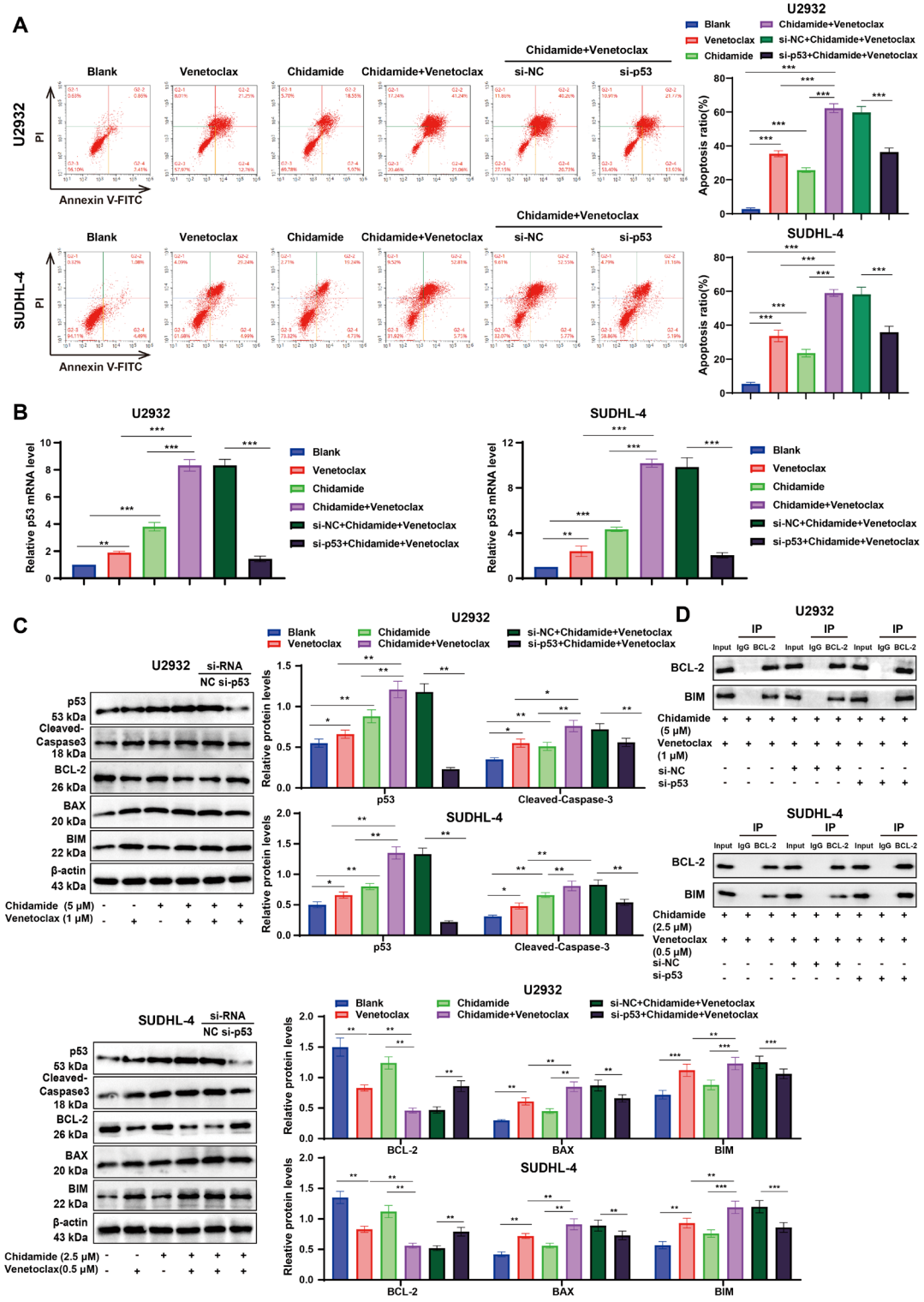

Figure 3. Assessment of apoptosis in DLBCL cells treated with chidamide and venetoclax. A) Flow cytometry was utilized to measure the rate of apoptosis in the treated cells. B) qRT-PCR was conducted to evaluate the expression of p53 in DLBCL cells following p53 knockdown. C) Western blot analysis was conducted to evaluate the expression of p53/apoptosis-related proteins in DLBCL cells following p53 knockdown. D) Co-IP assay was performed to assess the interaction between BCL-2 and BIM. All cellular experiments were performed in triplicate independently, with data presented as the mean ± standard deviation. Intergroup comparisons were conducted using one-way ANOVA, followed by Tukey's multiple comparisons test for post hoc analysis. Statistical significance was denoted as *p<0.05, **p<0.01, and ***p<0.001. Abbreviations: BAX-BCL-2-associated X protein; BIM-BCL2L11; BCL-2-B-cell lymphoma 2

3, while BCL-2 declined in DLBCL cells. When comparing the combined treatment to single-agent therapy, the expression levels of p53, BAX, and cleaved caspase 3 were significantly enhanced, but BCL-2 was remarkably decreased (all $p<0.01$) (Figure 3C). Subsequently, DLBCL cells were transfected with p53 siRNA and then subjected to combined treatment with chidamide and venetoclax for 24 h. qRT-PCR and western blot analyses confirmed the successful knockdown of p53 (Figures 3B, 3C). Furthermore, following silencing of p53, apoptosis in DLBCL cells was significantly reduced (all $p<0.01$), along with a notable decrease in the expression of BIM, BAX, and cleaved caspase 3, and a substantial increase in BCL-2 expression (all $p<0.01$) (Figure 3C). It has been reported that venetoclax disrupts the BCL-2-BIM interaction and promotes apoptosis of DH-DPL cells [24]. Consequently, the interaction between BCL-2 and BIM in cells following p53 knockdown was assessed using the co-IP assay. It was found that elevated BCL-2 protein levels contributed to enhanced BCL-2/BIM complex formation in the si-p53 cell line (Figure 3D). These findings suggest that the combined treatment of chidamide and venetoclax effectively induces apoptosis in DLBCL cells, while the downregulation of p53 expression can partially reverse the apoptotic effects of the combined treatment.

Upregulation of the p53-p21 pathway induced by the combination of chidamide and venetoclax results in G1/S phase cell cycle arrest in DLBCL cells. To further investigate the effects of the combination of chidamide and venetoclax on the cell cycle of DLBCL cell lines, we employed flow cytometry to evaluate cell cycle distribution. As illustrated in Figure 4A-B, relative to cells receiving no treatment, treatment with venetoclax had no significant effect on cell cycle, but treatment with chidamide and its combination with venetoclax contributed to a notable increase in the proportion of DLBCL cells in the G1/S phase, indicating that the cell cycle was predominantly arrested at the G1/S transition. Furthermore, the G1/S phase arrest was significantly more pronounced with the combination treatment than with chidamide alone ($p<0.01$). Western blot analysis was conducted on cell cycle-related proteins, including Cyclin E, Cdk2, and p21, demonstrating that treatment with chidamide and venetoclax led to an elevation in p21 protein level, accompanied by a reduction in Cyclin E and Cdk2 levels, when compared to cells receiving no treatment (Figures 4C, 4D). The alterations in protein expression were significantly greater with the combination treatment compared to monotherapy ($p<0.05$).

Additionally, it has been reported that p21 is a transcriptional target of p53 [25]. We conducted predictive analysis using the Jaspar database to identify potential binding sites of p53 within the p21 promoter region (Figure 4E). Dual-luciferase reporter assay demonstrated that co-transfection of the oe-p53 and p21-MUT plasmids did not result in a significant change in luciferase activity ($p > 0.05$), whereas co-transfection with the oe-p53 and p21-WT plasmids resulted in a significant increase in luciferase activity ($p<0.001$) (Figure 4F). A ChIP assay was conducted to evaluate the enrichment of p53 at the p21 promoter region. As shown in Figure 4G, treatment with chidamide led to a significant increase in p53 enrichment at the p21 promoter, and the combination treatment further enhanced this effect ($p<0.01$).

Inhibition of p21 partially reverses the regulatory effects of combination treatment with chidamide and venetoclax on cell cycle arrest and apoptosis in DLBCL cells. In this study, we utilized p21 siRNA to transfect DLBCL cells for 24 h, followed by treatment with chidamide and venetoclax for an additional 24 h. The results demonstrated a significant reduction in p21 expression levels within the DLBCL cells transfected with p21 siRNA (Figures 5A, 5B) (both $p<0.01$). Concurrently, cell apoptosis rate was markedly decreased (Figure 5C) ($p<0.001$), but cell proliferation was enhanced following p21 knockdown in DLBCL cells treated with chidamide and venetoclax, in addition to reduced apoptosis and notably alleviated G1/S phase cell cycle arrest (Figures 5D, 5E, 5G) (all $p<0.01$) led to a close G0/G1 value to that of control cells (Figures 4A, 4B) (all $p<0.01$). Furthermore, an increase was observed in the BCL-2 protein level, while the level of pro-apoptotic proteins BIM, BAX, and cleaved caspase 3 was significantly diminished in DLBCL cells treated with p21 siRNA, chidamide, and venetoclax (Figure 5F) (all $p<0.001$). Additionally, under this condition, the expression of cell cycle-related factors Cyclin E and Cdk2 was significantly elevated (Figure 5H) (all $p<0.001$) and the formation of the BCL-2/BIM complex was enhanced (Figure 5I). These findings indicate that the knockdown of p21 expression can partially reverse the regulatory effects of chidamide and venetoclax combination on cell cycle arrest and apoptosis in DLBCL cells.

Discussion

In this study, we demonstrated that the combined use of chidamide with venetoclax can induce the acetylation of histones H3 and H4 and promote p53 expression, thus resulting in cell cycle arrest and promoting cell apoptosis of DLBCL cells. Compared to treatment with chidamide or venetoclax alone, their combination treatment exerted synergistic effects on cell apoptosis and cell cycle arrest in U2932 (ABC subtype) and SUDHL-4 cells (GCB subtype). Therefore, the current study was conducted to explore the potential mechanisms underlying the synergistic effect of chidamide with venetoclax on promoting apoptosis of DLBCL cells, with the expectation of offering new insights into DLBCL treatment and clinical implications.

It has been reported that the GCB subtype DLBCL generally has a better prognosis than the ABC subtype [26]. In our research, SUDHL-4 cells also exhibited greater sensitivity to chidamide and venetoclax compared to U2932 cells, which is consistent with previously reported work [12]. Studies have shown that HDACis can reduce the expression of c-MYC by affecting chromatin structure,

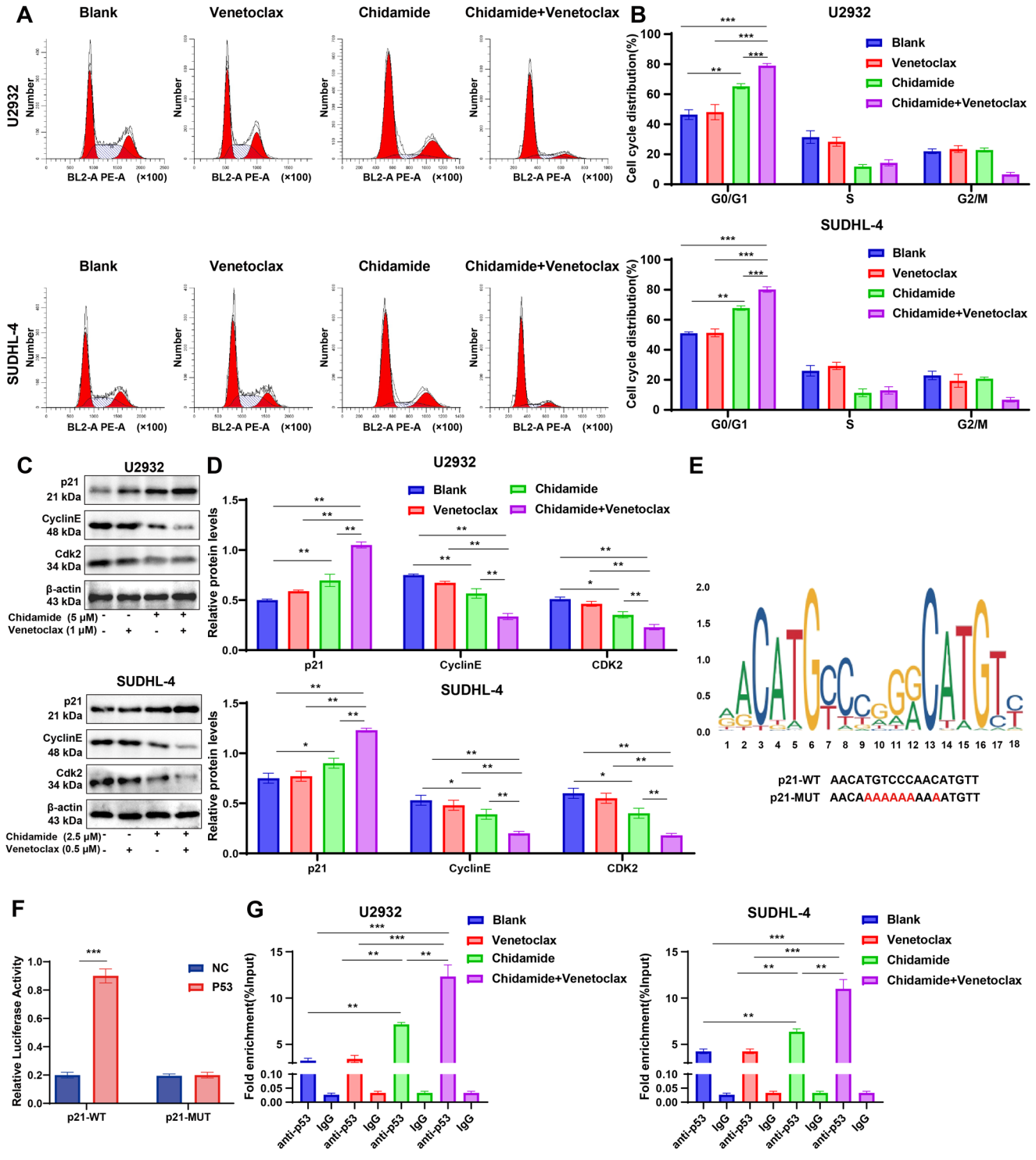

Figure 4. Cell cycle assessment and interaction between p53 and p21 following combination treatment. A, B) Flow cytometric analysis of cell cycle distribution. C, D) Western blot analysis of the expression of cell cycle-related proteins. E) Predicted binding sites of p53 in the p21 promoter region by the Jaspar database (https://jaspar.elixir.no/). F) Dual-luciferase reporter assay was conducted to assess the interaction between p53 and p21 by measuring firefly luciferase activity normalized to Renilla luciferase activity. G) A ChIP assay was conducted to determine the binding of p53 at the p21 promoter region. Cell experiments were conducted in triplicate independently, and data are presented as the mean ± standard deviation. For comparisons among multiple groups, one-way ANOVA was employed, followed by Tukey's multiple comparisons test; comparisons between two groups were performed using an independent samples t-test. *p<0.05, **p<0.01, and ***p<0.001. Abbreviations: p21-cyclin-dependent kinase inhibitor; Cyclin E-cyclin E; Cdk2-cyclin-dependent kinase 2; ChIP-chromatin immunoprecipitation

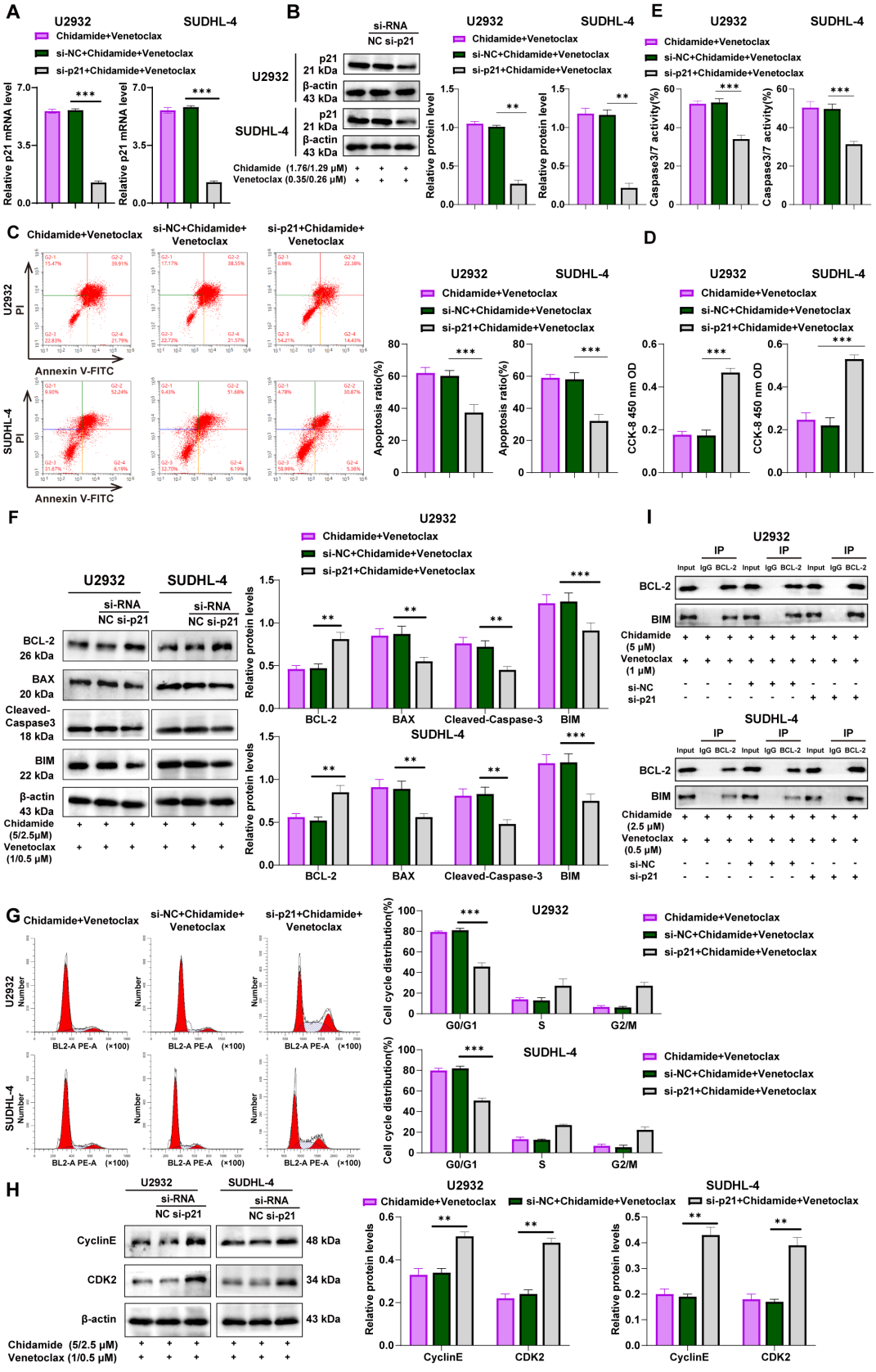

Figure 5. Role of p21 in cells treated with chidamide and venetoclax. A) qRT-PCR was conducted to evaluate the expression of p21 in cells with and without p21 knockdown. B) Western blot analysis to assess the expression level of p21 in cells with and without p21 knockdown. C) Flow cytometric analysis of apoptosis rates following p21 knockdown. D) CCK-8 assay was conducted to evaluate cell proliferation following p21 knockdown. E) Cell apoptosis was evaluated by the Caspase 3/7 Activity Apoptosis Assay Kit. F, H) Western blot detection of apoptosis-related proteins and cell cycle-associated proteins after p21 knockdown. G) Flow cytometric analysis of cell cycle distribution post p21 knockdown. I) Co-IP assay detection of the interaction between BCL-2 and BIM. Cell experiments were conducted in triplicate independently, and data are expressed as mean ± standard deviation. Between-group comparisons were performed using one-way ANOVA, followed by Tukey's multiple comparisons test. **p<0.01, and ***p<0.001. Abbreviations: p21-cyclin-dependent kinase inhibitor; Cyclin E-cyclin E; Cdk2-cyclin-dependent kinase 2; BAX-BCL-2-associated X protein; BIM-BCL2L11; BCL-2-B-cell lymphoma 2; Caspase 3/7-cysteine aspartase 3/7

thereby inhibiting cell proliferation and enhancing drug sensitivity [27–29]. As a crucial transcription factor, c-MYC is closely associated with tumorigenesis and drug resistance when overexpressed [29, 30]. Venetoclax has demonstrated the ability to displace the pro-apoptotic proteins that are bound to BCL-2, such as BIM, BAX, and BAK, leading to mitochondrial outer membrane permeabilization, cytochrome c release, and caspase activation, ultimately inducing apoptosis [31, 32]. Further, aberrant expression or mutations of MYC and BCL-2 genes in DLBCL cells is associated with the disease aggressiveness and resistance to some chemotherapeutic agents. Although neither SUDHL-4 cells nor U2932 cells carry MYC gene mutations [28, 33], the differences in chromosomal alterations and signaling pathway activation between GCB and ABC subtypes of DLBCL may contribute to higher drug sensitivity in SUDHL-4 than in U2932 [34, 35]. Besides, we also noted that the HDACi chidamide, by inhibiting HDAC activity, leads to increased p53 expression, a mechanism crucial for both chidamide monotherapy and combined therapy with the BCL-2 inhibitor venetoclax. HDACis are known to reverse post-translational deacetylation in cancer cells. It has also been demonstrated that HDACs interact with p53, inhibiting its acetylation and affecting its role in gene expression regulation [36]. HDACis can enhance p53 acetylation, increasing its transcriptional activity and inducing apoptosis in cancer cells [37, 38]. As a tumor suppressor, p53 activation promotes apoptosis of cancer cells [39]. In our study, chidamide treatment significantly suppressed HDAC activity in DLBCL cells, and its combination with venetoclax exhibited stronger inhibition of HDAC activity, leading to a more pronounced increase in p53 expression. Consistently, the current study also revealed that chidamide and venetoclax significantly induced apoptosis in DLBCL cells, while p53 knockdown partially reversed this effect. In conclusion, our study demonstrated that chidamide-induced inhibition of HDAC activity leads to increased p53 expression, and the therapeutic efficacy of chidamide, either as monotherapy or in combination with venetoclax, is dependent on p53 expression.

Further investigation on the effect of chidamide and venetoclax on the cell cycle of DLBCL cells demonstrated that the enrichment expression of p53 in the p21 promoter, highlighting the implication of the p53-p21 pathway in DLBCL cell apoptosis mediated by chidamide and venetoclax. As a crucial regulator of the cell cycle and apoptosis, p53 activates the downstream p21-CyclinE-Cdk2 signaling pathway, promoting apoptosis and inducing cell cycle arrest [40, 41]. Furthermore, p53 regulates the expression of p21 at the transcriptional level. There is evidence showing that p21, a cell cycle-dependent kinase inhibitor, blocks cell cycle progression and thereby suppresses cell proliferation [42, 43]. In this signaling pathway, p21 inhibits the activity of the CyclinE-Cdk2 complex, blocking the G1/S phase transition, further suppressing cell proliferation. The BCL-2 family proteins, which are key regulators of apoptosis, are broadly expressed in DLBCL cells, where their anti-apoptotic function is targeted by the BCL-2 inhibitor venetoclax [44]. Venetoclax promotes the permeabilization of the mitochondrial outer membrane by disengaging pro-apoptotic proteins BIM and BAX from BCL-2, which in turn activates apoptosis [45, 46]. BIM is a pro-apoptotic protein, and the amount of free BIM is decreased when BCL-2 binds with BIM to form the BCL-2/BIM complex [47]. BIM binds to the hydrophobic groove of BCL-2 via its BH3 domain, inducing conformational changes and forming a stable complex [48]. Following dissociation and release of BIM from BCL-2, the apoptotic cascade is initiated [49]. Venetoclax has been suggested to disrupt the BCL-2-BIM interaction to promote apoptosis of DH-DPL cells [24]. Our study data found that knockdown of p53 or p21 partially reversed the pro-apoptotic effect of chidamide combined with venetoclax on DLBCL cells, and increased the formation of the BCL-2/BIM complex. Chidamide, by upregulating p53 expression, further enhances the inhibitory effect of venetoclax on BCL-2, with their synergistic action markedly amplifying the apoptotic response of DLBCL cells. This synergy indicates that the combined use of venetoclax and chidamide plays a critical role in reducing anti-apoptotic signaling while enhancing cancer cell sensitivity to therapy via the p53-p21 pathway. A prior study has demonstrated that the combination of chidamide and venetoclax reduces the BCL-2/BIM ratio and decreases TP53 expression in DLBCL, thereby inhibiting DLBCL growth [21]. These data indicate that although the effects of HDACi in DLBCL all depend on the p53 pathway, their regulatory mechanisms are diverse and complex.

However, certain limitations remain in our study, such as the lack of further investigation into whether the synergistic effects of chidamide and venetoclax enhance drug sensitivity in resistant cell lines, and the absence of *in vivo* validation of combination therapy efficacy. Additionally, further exploration of other epigenetic mechanisms, such as DNA methylation and nucleosome positioning, will help elucidate the molecular mechanisms underlying the combination therapy of chidamide and venetoclax in DLBCL, providing insight into the feasibility of epigenetic inhibition in DLBCL treatment.

In summary, this study's findings suggest that the combination of the HDACi chidamide and the BCL-2 inhibitor venetoclax can regulate apoptosis and cell cycle arrest in DLBCL cells by the p53-p21-CyclinE-Cdk2 signaling pathway, offering a promising therapeutic strategy for DLBCL. Future research should focus on refining this mechanism and validating its clinical potential through *in vivo* studies, with the goal of achieving further breakthroughs in DLBCL treatment.

Acknowledgments: The study was financed under the provisions of the institutional budget.

References

[1] LEWIS KL, CHEAH CY. The value of bispecific antibodies in relapsed and refractory DLBCL. Leuk Lymphoma 2024; 65: 720–735. https://doi.org/10.1080/10428194.2024.2323085

[2] WENZL K, STOKES ME, NOVAK JP, BOCK AM, KHAN S et al. Multiomic analysis identifies a high-risk signature that predicts early clinical failure in DLBCL. Blood Cancer J 2024; 14: 100. https://doi.org/10.1038/s41408-024-01080-0

[3] MELANI C, LAKHOTIA R, PITTALUGA S, PHELAN JD, HUANG DW et al. Combination Targeted Therapy in Relapsed Diffuse Large B-Cell Lymphoma. N Engl J Med 2024; 390: 2143–2155. https://doi.org/10.1056/NEJMoa2401532

[4] HOGG SJ, BEAVIS PA, DAWSON MA, JOHNSTONE RW. Targeting the epigenetic regulation of antitumour immunity. Nat Rev Drug Discov 2020; 19: 776–800. https://doi.org/10.1038/s41573-020-0077-5

[5] LIANG G, OH TG, HAH N, TIRIAC H, SHI Y et al. Inhibiting stromal Class I HDACs curbs pancreatic cancer progression. Nat Commun 2023; 14: 7791. https://doi.org/10.1038/s41467-023-42178-6

[6] YANG FF, HU T, LIU JQ, YU XQ, MA LY. Histone deacetylases (HDACs) as the promising immunotherapeutic targets for hematologic cancer treatment. Eur J Med Chem 2023; 245: 114920. https://doi.org/10.1016/j.ejmech.2022.114920

[7] PARK E, LEE C, PARK J, LIU J, HONG J et al. Mitigating the BFL1-mediated antiapoptotic pathway in diffuse large B cell lymphoma by inhibiting HDACs. Leuk Lymphoma 2023; 64: 205–216. https://doi.org/10.1080/10428194.2022.2140282

[8] SUN K, ATOYAN R, BOREK MA, DELLAROCCA S, SAMSON ME et al. Dual HDAC and PI3K Inhibitor CUDC-907 Downregulates MYC and Suppresses Growth of MYC-dependent Cancers. Mol Cancer Ther 2017; 16: 285–299. https://doi.org/10.1158/1535-7163.MCT-16-0390

[9] SHAO J, YE Z, SHEN Z, LIU N, ZHANG L et al. Chidamide improves gefitinib treatment outcomes in NSCLC by attenuating recruitment and immunosuppressive function of myeloid-derived suppressor cells. Biomed Pharmacother 2024; 173: 116306. https://doi.org/10.1016/j.biopha.2024.116306

[10] ZHANG Y, CHEN Z, LIU Y, HAN L, JIANG W et al. Chidamide plus envafolimab as subsequent treatment in advanced non-small cell lung cancer patients resistant to anti-PD-1 therapy: A multicohort, open-label, phase II trial with biomarker analysis. Cancer Med 2024; 13: e7175. https://doi.org/10.1002/cam4.7175

[11] WU C, SONG Q, GAO S, WU S. Targeting HDACs for diffuse large B-cell lymphoma therapy. Sci Rep 2024; 14: 289. https://doi.org/10.1038/s41598-023-50956-x

[12] GUAN XW, WANG HQ, BAN WW, CHANG Z, CHEN HZ et al. Novel HDAC inhibitor Chidamide synergizes with Rituximab to inhibit diffuse large B-cell lymphoma tumour growth by upregulating CD20. Cell Death Dis 2020; 11: 20. https://doi.org/10.1038/s41419-019-2210-0

[13] GRABOW S, KELLY GL, DELBRIDGE AR, KELLY PN, BOUILLET P et al. Critical B-lymphoid cell intrinsic role of endogenous MCL-1 in c-MYC-induced lymphomagenesis. Cell Death Dis 2016; 7: e2132. https://doi.org/10.1038/cddis.2016.43

[14] ALFORD D, PETKOVIC I. Prognostic Significance of Bcl-2 Expression in Non-germinal Center B-cell-Like Diffuse Large B-cell Lymphoma. Cureus 2024; 16: e62031. https://doi.org/10.7759/cureus.62031

[15] DINARDO CD, JONAS BA, PULLARKAT V, THIRMAN MJ, GARCIA JS et al. Azacitidine and Venetoclax in Previously Untreated Acute Myeloid Leukemia. N Engl J Med 2020; 383: 617–629. https://doi.org/10.1056/NEJMoa2012971

[16] ROBERTS AW, WEI AH, HUANG DCS. BCL2 and MCL1 inhibitors for hematologic malignancies. Blood 2021; 138: 1120–1136. https://doi.org/10.1182/blood.2020006785

[17] LIU J, LI S, WANG Q, FENG Y, XING H et al. Sonrotoclax overcomes BCL2 G101V mutation-induced venetoclax resistance in preclinical models of hematologic malignancy. Blood 2024; 143: 1825–1836. https://doi.org/10.1182/blood.2023019706

[18] DESAI A, PETERS S. Immunotherapy-based combinations in metastatic NSCLC. Cancer Treat Rev 2023; 116: 102545. https://doi.org/10.1016/j.ctrv.2023.102545

[19] GEANES ES, KREPEL SA, MCLENNAN R, PIERCE S, KHANAL S et al. Development of combinatorial antibody therapies for diffuse large B cell lymphoma. Front Med (Lausanne) 2022; 9: 1034594. https://doi.org/10.3389/fmed.2022.1034594

[20] SCHUSTER M, ZIJLSTRA J, CASASNOVAS RO, VERMAAT JSP, KALAKONDA N et al. Effect of Prior Therapy and Disease Refractoriness on the Efficacy and Safety of Oral Selinexor in Patients with Diffuse Large B-cell Lymphoma (DLBCL): A Post-hoc Analysis of the SADAL Study. Clin Lymphoma Myeloma Leuk 2022; 22: 483–494. https://doi.org/10.1016/j.clml.2021.12.016

[21] LUO C, YU T, YOUNG KH, YU L. HDAC inhibitor chidamide synergizes with venetoclax to inhibit the growth of diffuse large B-cell lymphoma via down-regulation of MYC, BCL2, and TP53 expression. J Zhejiang Univ Sci B 2022; 23: 666–681. https://doi.org/10.1631/jzus.B2200016

[22] CHOU T, MARTIN N. CompuSyn software. CompuSyn for drug combinations: PC software and user's guide: a computer program for quantitation of synergism and antagonism in drug combinations, and the determination of IC50 and ED50 and LD50 values. ComboSyn Inc., Paramus, NJ. 2005. https://www.combosyn.com

[23] ZHAO S, GUO J, ZHAO Y, FEI C, ZHENG Q et al. Chidamide, a novel histone deacetylase inhibitor, inhibits the viability of MDS and AML cells by suppressing JAK2/STAT3 signaling. Am J Transl Res 2016; 8: 3169–3178.

[24] UCHIDA A, ISOBE Y, ASANO J, UEMURA Y, HOSHIKAWA M et al. Targeting BCL2 with venetoclax is a promising therapeutic strategy for "double-protein expression" lymphoma with MYC and BCL2 rearrangements. Haematologica 2019; 104: 1417–1421. https://doi.org/10.3324/haematol.2018.204958

[25] LEVINE AJ. p53: 800 million years of evolution and 40 years of discovery. Nat Rev Cancer 2020; 20: 471–480. https://doi.org/10.1038/s41568-020-0262-1

[26] LENZ G, STAUDT LM. Aggressive lymphomas. N Engl J Med 2010; 362: 1417–1429. https://doi.org/10.1056/NEJMra0807082

[27] NEBBIOSO A, CARAFA V, CONTE M, TAMBARO FP, ABBONDANZA C et al. c-Myc Modulation and Acetylation Is a Key HDAC Inhibitor Target in Cancer. Clin Cancer Res 2017; 23: 2542–2555. https://doi.org/10.1158/1078-0432.CCR-15-2388

[28] LI W, GUPTA SK, HAN W, KUNDSON RA, NELSON S et al. Targeting MYC activity in double-hit lymphoma with MYC and BCL2 and/or BCL6 rearrangements with epigenetic bromodomain inhibitors. J Hematol Oncol 2019; 12: 73. https://doi.org/10.1186/s13045-019-0761-2

[29] ECKER J, THATIKONDA V, SIGISMONDO G, SELT F, VALINCIUTE G et al. Reduced chromatin binding of MYC is a key effect of HDAC inhibition in MYC amplified medulloblastoma. Neuro Oncol 2021; 23: 226–239. https://doi.org/10.1093/neuonc/noaa191

[30] BARRANS S, CROUCH S, SMITH A, TURNER K, OWEN R et al. Rearrangement of MYC is associated with poor prognosis in patients with diffuse large B-cell lymphoma treated in the era of rituximab. J Clin Oncol 2010; 28: 3360–3365. https://doi.org/10.1200/JCO.2009.26.3947

[31] NACHMIAS B, AUMANN S, HARAN A, SCHIMMER AD. Venetoclax resistance in acute myeloid leukaemia-Clinical and biological insights. Br J Haematol. 2024; 204: 1146-1158.

[32] BHOLA PD, LETAI A. Mitochondria-Judges and Executioners of Cell Death Sentences. Mol Cell 2016; 61: 695–704. https://doi.org/10.1016/j.molcel.2016.02.019

[33] KARMALI R, CHUKKAPALLI V, GORDON LI, BORGIA JA, UGOLKOV A et al. GSK-3beta inhibitor, 9-ING-41, reduces cell viability and halts proliferation of B-cell lymphoma cell lines as a single agent and in combination with novel agents. Oncotarget 2017; 8: 114924–114934. https://doi.org/10.18632/oncotarget.22414

[34] YOUNG RM, SHAFFER AL 3RD, PHELAN JD, STAUDT LM. B-cell receptor signaling in diffuse large B-cell lymphoma. Semin Hematol 2015; 52: 77–85. https://doi.org/10.1053/j.seminhematol.2015.01.008

[35] Wang J, Zhao AL, Li H, Yang LY, Chen LJ et al. [In vitro pharmacodynamic studies of novel class I and IIb selective histone deacetylase inhibitor purinostat mesylate in the treatment of diffuse large B-cell lymphoma and its mechanism]. Zhonghua Xue Ye Xue Za Zhi 2022; 43: 753–759. https://doi.org/10.3760/cma.j.issn.0253-2727.2022.09.007

[36] CELESIA A, FRANZO M, DI LIBERTO D, LAURICELLA M, CARLISI D et al. Oncogenic BRAF and p53 Interplay in Melanoma Cells and the Effects of the HDAC Inhibitor ITF2357 (Givinostat). Int J Mol Sci 2023; 24: 9148. https://doi.org/10.3390/ijms24119148

[37] BENJAMIN DI, BOTH P, BENJAMIN JS, NUTTER CW, TAN JH et al. Fasting induces a highly resilient deep quiescent state in muscle stem cells via ketone body signaling. Cell Metab 2022; 34: 902–18e6. https://doi.org/10.1016/j.cmet.2022.04.012

[38] HU Y, DAI J, ZONG G, XIAO J, GUO X et al. Restoration of p53 acetylation by HDAC inhibition permits the necrosis/apoptosis switch of pancreatic acinar cell during experimental pancreatitis in mice. J Cell Physiol 2019; 234: 21988–21998. https://doi.org/10.1002/jcp.28761

[39] LIU Y, SU Z, TAVANA O, GU W. Understanding the complexity of p53 in a new era of tumor suppression. Cancer Cell 2024; 42: 946–967. https://doi.org/10.1016/j.ccell.2024.04.009

[40] GHOSH M, SAHA S, LI J, MONTROSE DC, MARTINEZ LA. p53 engages the cGAS/STING cytosolic DNA sensing pathway for tumor suppression. Mol Cell 2023; 83: 266–80e6. https://doi.org/10.1016/j.molcel.2022.12.023

[41] MARVALIM C, DATTA A, LEE SC. Role of p53 in breast cancer progression: An insight into p53 targeted therapy. Theranostics 2023; 13: 1421–1442. https://doi.org/10.7150/thno.81847

[42] WU T, YANG Z, CHEN W, JIANG M, XIAO Z et al. miR-30e-5p-mediated FOXD1 promotes cell proliferation by blocking cellular senescence and apoptosis through p21/CDK2/Rb signaling in head and neck carcinoma. Cell Death Discov 2023; 9: 295. https://doi.org/10.1038/s41420-023-01571-2

[43] ENGELAND K. Cell cycle regulation: p53-p21-RB signaling. Cell Death Differ 2022; 29: 946–960. https://doi.org/10.1038/s41418-022-00988-z

[44] ZHOU Z, ZHANG L, WANG X, LI X, LI L et al. Ibrutinib combined with venetoclax for the treatment of relapsed/refractory diffuse large B cell lymphoma. Ann Hematol 2021; 100: 1509–1516. https://doi.org/10.1007/s00277-021-04535-7

[45] CHONG SJF, ZHU F, DASHEVSKY O, MIZUNO R, LAI JX et al. Hyperphosphorylation of BCL-2 family proteins underlies functional resistance to venetoclax in lymphoid malignancies. J Clin Invest 2023; 133: e170169. https://doi.org/10.1172/JCI170169

[46] ZHU F, CROMBIE JL, NI W, HOANG NM, GARG S et al. Hypomethylating agent decitabine sensitizes diffuse large B-cell lymphoma to venetoclax. Haematologica 2024; 109: 186-199. https://doi.org/10.3324/haematol.2023.283245

[47] JIANG X, JIANG H, SHEN Z, WANG X. Activation of mitochondrial protease OMA1 by Bax and Bak promotes cytochrome c release during apoptosis. Proc Natl Acad Sci U S A 2014; 111: 14782–14787. https://doi.org/10.1073/pnas.1417253111

[48] HINDS MG, SMITS C, FREDERICKS-SHORT R, RISK JM, BAILEY M et al. Bim, Bad and Bmf: intrinsically unstructured BH3-only proteins that undergo a localized conformational change upon binding to prosurvival Bcl-2 targets. Cell Death Differ 2007; 14: 128–136. https://doi.org/10.1038/sj.cdd.4401934

[49] UTHALE A, ANANTRAM A, SULKSHANE P, DEGANI M, TENI T. Identification of bicyclic compounds that act as dual inhibitors of Bcl-2 and Mcl-1. Mol Divers 2023; 27: 1359–1374. https://doi.org/10.1007/s11030-022-10494-6